Upper Bound on the Decay $\tau \to \mu\gamma$ from the Belle Detector

K. Abe,[6] K. Abe,[38] T. Abe,[6] I. Adachi,[6] Byoung Sup Ahn,[13] H. Aihara,[40] K. Akai,[6] M. Akatsu,[19] M. Akemoto,[6] Y. Asano,[45] T. Aso,[44] V. Aulchenko,[1] T. Aushev,[10] A. M. Bakich,[35] Y. Ban,[30] S. Banerjee,[36] A. Bay,[15] I. Bedny,[1] I. Bizjak,[11] A. Bondar,[1] A. Bozek,[24] M. Bračko,[17,11] T. E. Browder,[5] Y. Chao,[23] K.-F. Chen,[23] B. G. Cheon,[34] R. Chistov,[10] S.-K. Choi,[4] Y. Choi,[34] Y. K. Choi,[34] A. Chuvikov,[31] M. Danilov,[10] L. Y. Dong,[8] A. Drutskoy,[10] S. Eidelman,[1] V. Eiges,[10] Y. Enari,[19] J. Flanagan,[6] C. Fukunaga,[42] K. Furukawa,[6] N. Gabyshev,[6] A. Garmash,[1,6] T. Gershon,[6] R. Guo,[21] J. Haba,[6] C. Hagner,[47] F. Handa,[39] H. Hayashii,[20] M. Hazumi,[6] T. Hokuue,[19] Y. Hoshi,[38] W.-S. Hou,[23] H.-C. Huang,[23] T. Iijima,[19] H. Ikeda,[6] K. Inami,[19] A. Ishikawa,[19] R. Itoh,[6] H. Iwasaki,[6] M. Iwasaki,[40] Y. Iwasaki,[6] J. H. Kang,[49] J. S. Kang,[13] N. Katayama,[6] H. Kawai,[2] T. Kawasaki,[26] H. Kichimi,[6] E. Kikutani,[6] H. J. Kim,[49] J. H. Kim,[34] S. K. Kim,[33] K. Kinoshita,[3] P. Koppenburg,[6] S. Korpar,[17,11] P. Krokovny,[1] R. Kulasiri,[3] A. Kuzmin,[1] Y.-J. Kwon,[49] S. H. Lee,[33] T. Lesiak,[24] J. Li,[32] A. Limosani,[18] S.-W. Lin,[23] D. Liventsev,[10] F. Mandl,[9] T. Matsumoto,[42] A. Matyja,[24] S. Michizono,[6] T. Mimashi,[6] W. Mitaroff,[9] K. Miyabayashi,[20] H. Miyata,[26] D. Mohapatra,[47] T. Mori,[41] T. Nagamine,[39] Y. Nagasaka,[7] T. T. Nakamura,[6] E. Nakano,[27] M. Nakao,[6] H. Nakazawa,[6] Z. Natkaniec,[24] S. Nishida,[6] O. Nitoh,[43] S. Ogawa,[37] Y. Ogawa,[6] K. Ohmi,[6] Y. Ohnishi,[6] T. Ohshima,[19] N. Ohuchi,[6] T. Okabe,[19] S. Okuno,[12] W. Ostrowicz,[24] H. Ozaki,[6] H. Palka,[24] C.W. Park,[13] H. Park,[14] N. Parslow,[35] L. E. Piilonen,[47] N. Root,[1] H. Sagawa,[6] S. Saitoh,[6] Y. Sakai,[6] M. Satapathy,[46] A. Satpathy,[6,3] O. Schneider,[15] J. Schümann,[23] A. J. Schwartz,[3] S. Semenov,[10] K. Senyo,[19] R. Seuster,[5] M. E. Sevior,[18] H. Shibuya,[37] T. Shidara,[6] B. Shwartz,[1] V. Sidorov,[1] J. B. Singh,[29] N. Soni,[29] S. Stanič,[45,*] M. Starič,[11] A. Sugi,[19] K. Sumisawa,[28] T. Sumiyoshi,[42] S. Suzuki,[48] S. Y. Suzuki,[6] F. Takasaki,[6] K. Tamai,[6] N. Tamura,[26] M. Tanaka,[6] M. Tawada,[6] G. N. Taylor,[18] Y. Teramoto,[27] T. Tomura,[40] T. Tsuboyama,[6] T. Tsukamoto,[6] S. Uehara,[6] K. Ueno,[23] S. Uno,[6] G. Varner,[5] C. C. Wang,[23] C. H. Wang,[22] J. G. Wang,[47] Y. Watanabe,[41] E. Won,[13] B. D. Yabsley,[47] Y. Yamada,[6] A. Yamaguchi,[39] Y. Yamashita,[25] M. Yamauchi,[6] H. Yanai,[26] Heyoung Yang,[33] M. Yoshida,[6] Y. Yusa,[39] Z. P. Zhang,[32] Y. Zheng,[5] V. Zhilich,[1] and D. Žontar[16,11]

(Belle Collaboration)

[1]*Budker Institute of Nuclear Physics, Novosibirsk*
[2]*Chiba University, Chiba*
[3]*University of Cincinnati, Cincinnati, Ohio 45221*
[4]*Gyeongsang National University, Chinju*
[5]*University of Hawaii, Honolulu, Hawaii 96822*
[6]*High Energy Accelerator Research Organization (KEK), Tsukuba*
[7]*Hiroshima Institute of Technology, Hiroshima*
[8]*Institute of High Energy Physics, Chinese Academy of Sciences, Beijing*
[9]*Institute of High Energy Physics, Vienna*
[10]*Institute for Theoretical and Experimental Physics, Moscow*
[11]*J. Stefan Institute, Ljubljana*
[12]*Kanagawa University, Yokohama*
[13]*Korea University, Seoul*
[14]*Kyungpook National University, Taegu*
[15]*Institut de Physique des Hautes Énergies, Université de Lausanne, Lausanne*
[16]*University of Ljubljana, Ljubljana*
[17]*University of Maribor, Maribor*
[18]*University of Melbourne, Victoria*
[19]*Nagoya University, Nagoya*
[20]*Nara Women's University, Nara*
[21]*National Kaohsiung Normal University, Kaohsiung*
[22]*National Lien-Ho Institute of Technology, Miao Li*
[23]*Department of Physics, National Taiwan University, Taipei*
[24]*H. Niewodniczanski Institute of Nuclear Physics, Krakow*
[25]*Nihon Dental College, Niigata*
[26]*Niigata University, Niigata*
[27]*Osaka City University, Osaka*
[28]*Osaka University, Osaka*
[29]*Panjab University, Chandigarh*

 0031-9007/04/92(17)/171802(6)$22.50

[30]*Peking University, Beijing*
[31]*Princeton University, Princeton, New Jersey 08545*
[32]*University of Science and Technology of China, Hefei*
[33]*Seoul National University, Seoul*
[34]*Sungkyunkwan University, Suwon*
[35]*University of Sydney, Sydney, New South Wales*
[36]*Tata Institute of Fundamental Research, Bombay*
[37]*Toho University, Funabashi*
[38]*Tohoku Gakuin University, Tagajo*
[39]*Tohoku University, Sendai*
[40]*Department of Physics, University of Tokyo, Tokyo*
[41]*Tokyo Institute of Technology, Tokyo*
[42]*Tokyo Metropolitan University, Tokyo*
[43]*Tokyo University of Agriculture and Technology, Tokyo*
[44]*Toyama National College of Maritime Technology, Toyama*
[45]*University of Tsukuba, Tsukuba*
[46]*Utkal University, Bhubaneswer*
[47]*Virginia Polytechnic Institute and State University, Blacksburg, Virginia 24061*
[48]*Yokkaichi University, Yokkaichi*
[49]*Yonsei University, Seoul*

(Received 14 October 2003; published 29 April 2004)

We have performed a search for the lepton-flavor-violating decay $\tau \to \mu\gamma$ using a data sample of 86.3 fb^{-1} accumulated by the Belle detector at KEK. No evidence for a signal is seen, and we set an upper limit for the branching fraction of $\mathcal{B}(\tau \to \mu\gamma) < 3.1 \times 10^{-7}$ at the 90% confidence level.

DOI: 10.1103/PhysRevLett.92.171802 PACS numbers: 13.35.Dx, 11.30.Fs, 14.60.Fg

The decay $\tau \to \mu\gamma$ violates lepton flavor conservation and is forbidden within the standard model (SM). However, some supersymmetric models, left-right symmetric models, and others [1] predict a branching fraction in the range of 10^{-7} to 10^{-9}, which is accessible at an e^+e^- B factory. It is notable that $\mathcal{B}(\tau \to \mu\gamma)$ could be enhanced by a factor of 10^5–10^6 relative to $\mathcal{B}(\mu \to e\gamma)$, because relevant kinematical factors depend on powers of m_τ/m_μ. The decay $\tau \to \mu\gamma$ is thus a promising process in which to search for new physics.

This decay has previously been searched for by the following Collaborations: Mark II [2], ARGUS [3], DELPHI [4], CLEO [5,6], and BaBar [7]. The most sensitive upper limit, reported by the CLEO Collaboration, is $\mathcal{B}(\tau \to \mu\gamma) < 1.1 \times 10^{-6}$ at 90% C.L.

We present here our study using 86.3 fb^{-1} of data collected at the $\Upsilon(4S)$ resonance with the Belle detector at the KEKB asymmetric e^+e^- collider [8]. A description of the detector can be found in Ref. [9].

We search for an event composed of exactly two oppositely charged tracks and at least one photon candidate, which is consistent with a $\tau^+\tau^-$ event in which one τ decays to $\mu\gamma$ and the other τ decays to a nonmuon charged particle, neutrino(s) and any number of γ's.

The selection criteria are determined by examining Monte Carlo (MC) simulations for signal τ-pair decay and background events (BG), such as generic τ-pair decay ($\tau^+\tau^-$), $q\bar{q}$ continuum, $B\overline{B}$, Bhabha scattering, and $\mu^+\mu^-$ as well as two-photon processes. The KORALB/TAUOLA [10] and QQ [11] generators are used for event generation, and GEANT3 [12] is used to simulate the Belle detector. The two-body decay $\tau \to \mu\gamma$ is initially assumed to have a uniform angular distribution in the τ's rest system; possible deviations from this are considered later.

The selection criteria are chosen to maximize the signal sensitivity. Kinematic variables with a c.m. superscript are calculated in the center-of-mass frame; all other variables are calculated in the laboratory frame. Each track is required to have momentum $p^{CM} < 4.5$ GeV/c and momentum transverse to the e^+ beam $p_t \geq 0.1$ GeV/c. Both tracks are required to be within the acceptance of a muon identification system (KLM): $-0.819 < \cos\theta < 0.906$, where θ is the polar angle with respect to the e^+ beam direction. Muon candidates are identified via a muon relative likelihood $\mathcal{L}_\mu$ [13], which is based on the difference between the range calculated from the particle momentum and the range measured by the KLM. It also includes the χ^2 formed from the KLM hit locations with respect to the extrapolated track. The charged track that forms a $\tau \to \mu\gamma$ candidate is required to have $p > 1.0$ GeV/c and $\mathcal{L}_\mu > 0.95$. The other track (on the "tag-side") is required to have $\mathcal{L}_\mu < 0.80$; i.e., we require that it not be a muon to reduce $e^+e^- \to \mu^+\mu^-\gamma$ background (γ from initial-state radiation). The fraction of muons with $\mathcal{L}_\mu < 0.80$ is denoted as η and is measured to be (for a tagside muon) $(12 \pm 3)\%$.

Photon candidates, whose definition is given in Ref. [14], are required to be within the acceptance of an electromagnetic calorimeter (ECL): $-0.866 < \cos\theta_\gamma < 0.906$. The photon that forms a $\tau \to \mu\gamma$ candidate is required to have an energy $E_\gamma > 0.5$ GeV in order to

avoid a spurious combination of a low-energy γ with the muon.

A cut $E^{CM}_{\rm sum} < 9.0$ GeV is imposed to reject Bhabha scattering and $\mu^+\mu^-$ production, where $E^{CM}_{\rm sum}$ is defined as the sum of the energies of the two charged tracks and the photon composing the $\mu\gamma$. A restriction on the opening angle between the μ and γ, $0.4 < \cos\theta^{CM}_{\mu-\gamma} < 00.8$, is particularly powerful to reject background events arising mostly from $e^+e^- \to \tau^+\tau^-$, $\tau \to \pi^0 X$. This process forms the backward peak in the open histogram in Fig. 1(a). The opening angle between the two tracks is required to be greater than 90°.

We define $\vec{p}_{\rm miss}$ as the residual momentum vector calculated by subtracting the vector sum of all visible momenta (from tracks and photon candidates) from the sum of the e^+ and e^- beam momenta. We include all photon candidates with energy greater than 0.1 GeV in the $p_{\rm miss}$ calculation. Constraints on the momentum and polar angle of the missing particle(s), $p_{\rm miss} > 0.4$ GeV/c and $-0.866 < \cos\theta_{\rm miss} < 0.956$, respectively, are imposed to increase the probability that the missing particle(s) is an undetected neutrino(s) rather than γ's or charged particles falling outside the acceptance of the detector. To remove $\tau^+\tau^-$ events, we apply a requirement to the opening angle between the tagging track and the missing particle, $\cos\theta^{\rm CM}_{\rm tag\text{-}miss} > 0.4$, as shown in Fig. 1(b).

Next, a condition is imposed on the relation between $p_{\rm miss}$ and the mass squared of a missing particle ($m^2_{\rm miss}$). The latter is defined as $E^2_{\rm miss} - p^2_{\rm miss}$, where $E_{\rm miss}$ is 11.5 GeV (the sum of the beam energies) minus the sum of all visible energy and is calculated assuming the muon (pion) mass for the charged track on the signal (tag) side. We require $p_{\rm miss} > -5 \times m^2_{\rm miss} - 1$ and $p_{\rm miss} > 1.5 \times m^2_{\rm miss} - 1$, where $p_{\rm miss}$ is in GeV/c and $m_{\rm miss}$ is in GeV/c^2. This cut loses 24% of the signal but removes 98% of the remaining $\tau^+\tau^-$ background (see Fig. 2) and 86% of the $\mu^+\mu^-$ background.

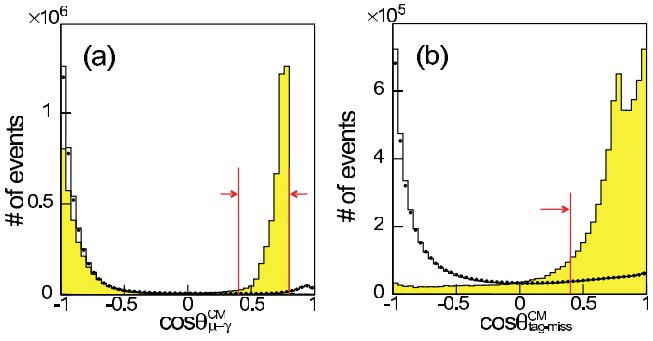

FIG. 1 (color online). Distributions of the opening angle between (a) the μ and γ on the signal side, and (b) the tagging track and the missing momentum. MC distributions for signal and $\tau^+\tau^-$ events are indicated by shaded and open histograms, respectively, and data by closed circles. The arrows show the selected ranges.

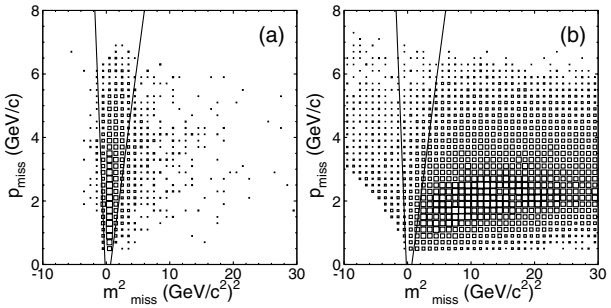

FIG. 2. Distribution of events in the $m^2_{\rm miss}$-$p_{\rm miss}$ plane. The selection boundary is indicated by two lines for (a) signal MC events and (b) $\tau^+\tau^-$ MC events.

After these selection requirements, 713 events remain in the data without any restriction on the mass and momentum of the $\mu\gamma$ system. The detection efficiency is evaluated by MC to be $\epsilon = 12.0 \pm 0.1\%$.

The candidate $\mu\gamma$ system should have an invariant mass ($M_{\rm inv}$) close to the τ lepton mass and an energy close to the beam energy in the c.m. frame; i.e., $\Delta E = E^{CM}_{\mu\gamma} - E^{CM}_{\rm beam} \simeq 0$. When deciding on our selection criteria, we excluded the signal region 1.70 GeV/$c^2 < M_{\rm inv} < 1.85$ GeV/c^2 so as not to bias our choice of criteria (a "blind" analysis). Only after all cuts were finalized and the number of background events estimated did we include this region and count the number of signal events. The resultant ΔE vs $M_{\rm inv}$ plot is shown in Fig. 3. For comparison, the equivalent plot for MC $\tau \to \mu\gamma$ decays is also shown. Because of the photon's energy leakage from the ECL detector and initial-state radiation, the MC

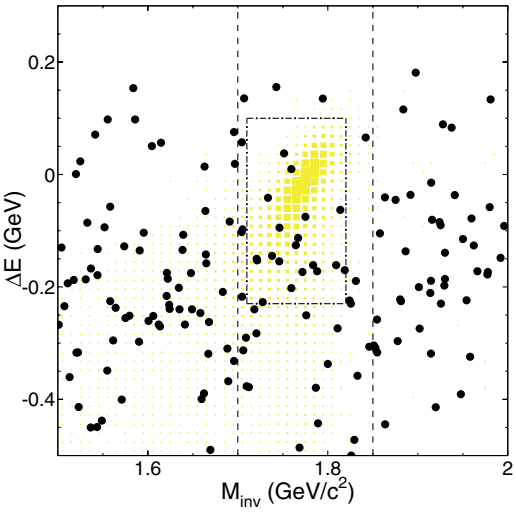

FIG. 3 (color online). Remaining events in data (circles) and the expected density for signal MC events (shaded) in the ΔE-$M_{\rm inv}$ plane. The region between the dashed lines is kept excluded until the selection criteria are finalized and the expected background estimated. The signal box (defined in the text) is indicated by a dash-dotted box.

simulation exhibits a long low-energy tail across the ΔE-$M_{\rm inv}$ plane. The individual ΔE and $M_{\rm inv}$ distributions around the peak are reproduced by asymmetric Gaussians with $\sigma_{\Delta E}^{\rm low/high} = (75.4 \pm 0.7)/(33.7 \pm 0.4)$ MeV and $\sigma_{M_{\rm inv}}^{\rm low/high} = (23.1 \pm 1.2)/(15.0 \pm 0.6)$ MeV$/c^2$, where $\sigma^{\rm low/high}$ means the standard deviation at the lower/higher side of the peak. The peak positions are -1.1 ± 0.5 MeV and 1776.8 ± 1.0 MeV$/c^2$ for ΔE and $M_{\rm inv}$, respectively.

We define a ΔE-$M_{\rm inv}$ region to evaluate the number of signal candidates. The signal box is defined as the area within $\pm 3\sigma$ for both ΔE and $M_{\rm inv}$: -0.23 GeV $< \Delta E <$ 0.10 GeV and 1.71 GeV$/c^2 < M_{\rm inv} <$ 1.82 GeV$/c^2$. The acceptance (Ω) for signal events passing all previous cuts is 87.3%.

There are two dominant sources of background: $e^+e^- \to \mu^+\mu^-\gamma$ and $e^+e^- \to \tau^+\tau^-\gamma$, in which the photon is radiated from the initial state. In the former case the muon on the tagside is misidentified; in the latter case the muon on the signal side originates from $\tau \to \mu\nu\overline{\nu}$ decay. We hereafter denote the former background as $\not{\mu}\mu\gamma$ and the latter as $\tau\tau\gamma$. The $\tau\tau\gamma$ background is studied using a 150 fb^{-1} sample of MC $\tau^+\tau^-$ events. The $\not{\mu}\mu\gamma$ background is studied using data by requiring that both tracks be muons and applying the muon inefficiency (η) to the tagside track. For this selection, the signal (tag)-side muon is required to have $\mathcal{L}_\mu > 0.95(0.80)$. Within the whole ΔE-$M_{\rm inv}$ region shown in Fig. 3, the $\tau\tau\gamma$ process yields 90.6 ± 7.2 events and the $\not{\mu}\mu\gamma$ process 43.4 ± 12.4 events. Among the other background processes mentioned above, only the continuum background yields a nonnegligible contribution (12.7 ± 5.7 events). This background has a rather large uncertainty as it is evaluated using an MC sample corresponding to only 34 fb^{-1}. The expected backgrounds amount to 143.7 ± 15.5 events in total, where 3.0 events in the $\not{\mu}\mu\gamma$ sample that are estimated to originate from $\tau\tau\gamma$ are subtracted to avoid double counting. The number of data events in this region (now including the previously excluded region) after all selection cuts is 160 ± 13. This yield is consistent with the background estimate.

The distributions of $\tau\tau\gamma$ and $\not{\mu}\mu\gamma$ background events, $N^{\tau\tau\gamma}(M_{\rm inv}, \Delta E)$ and $N^{\not{\mu}\mu\gamma}(M_{\rm inv}, \Delta E)$, exhibit different behavior in ΔE. The former populates only the negative ΔE region, while the latter is distributed mostly in the positive ΔE region. Both types of background events, however, exhibit a similar correlation in the ΔE-$M_{\rm inv}$ plane and are empirically reproduced by a combination of Landau and Gaussian functions in ΔE, and a linear function in $M_{\rm inv}$. The background distribution can then be represented by the sum of two BG components as

$$N_{BG}(M_{\rm inv}, \Delta E) = N^{\tau\tau\gamma}(M_{\rm inv}, \Delta E) \times (1 + \Lambda) + N^{\mu/\mu\gamma}(M_{\rm inv}, \Delta E) \times \kappa, \quad (1)$$

where Λ is the continuum background contribution. This distribution is taken to be similar to that of $\tau\tau\gamma$, as indicated by Monte Carlo simulation. The factors $(1 + \Lambda)$ and $\kappa \equiv \eta/(1 - \eta)$ are 1.14 ± 0.09 and 0.14 ± 0.04, respectively, where the former is obtained from MC simulation and the latter is obtained by measuring the muon inefficiency (η) for $e^+e^- \to \mu^+\mu^-$ events.

The above background parametrization is compared with the data outside of the excluded region. Fitting the background shape to the data gives $1 + \Lambda = 1.22 \pm 0.13$ and $\kappa = 0.11 \pm 0.03$, which agree well with the values given above. For both sets of $1 + \Lambda$ and κ values, Figure 4 shows the expected background events $N_{BG}(M_{\rm inv}, \Delta E)$ as a function of ΔE for 1.71 GeV$/c^2 < M_{\rm inv} <$ 1.82 GeV$/c^2$. No appreciable difference is seen between the two $N_{BG}(M_{\rm inv}, \Delta E)$ distributions, and we take the latter values for $1 + \Lambda$ and κ. As the background has a linear (and in fact small) dependence on $M_{\rm inv}$, the amount of background in the signal region can be estimated by averaging the number of events counted in the $M_{\rm inv}$ sidebands 1.553–1.663 and 1.850–1.960 GeV$/c^2$. These sidebands begin a distance $2\sigma_{M_{\rm inv}}$ from the edges of the signal region so that no potential signal biases this estimate. When the events in the signal box are included, the data event distribution is found to match the expected $N_{BG}(M_{\rm inv}, \Delta E)$ well (see Fig. 4). Within the signal box, 19 events are found in the data while 20.2 ± 2.1 events are expected from Eq. (1) and 20.5 ± 6.4 events from the average of $M_{\rm inv}$ sidebands.

An upper limit is obtained using the most frequent method described in Refs. [6,15]. The likelihood function is defined as

$$\mathcal{L} = \frac{e^{-(s+b)}}{N!} \prod_{i=1}^{N} (sS_i + bB_i), \quad (2)$$

where N is the number of observed events, and s and b are the number of signal events and background events,

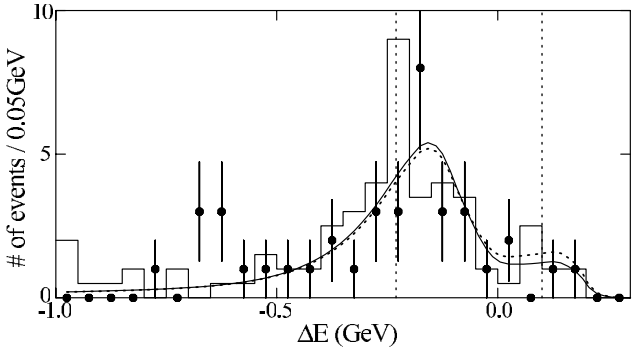

FIG. 4. ΔE distributions in the signal region, 1.71 GeV$/c^2 <$ $M_{\rm inv} <$ 1.82 GeV$/c^2$. The expected background is indicated by the solid (dashed) curve for $1 + \Lambda = 1.22(1.14)$ and $\kappa =$ 0.11(0.14). The histogram is an average of both sideband spectra. The data are the points with error bars. The vertical dashed lines indicate the ΔE range of the signal box.

respectively. S_i and B_i are the signal and background probability density functions, where i indicates the ith event. S_i is obtained by generating 100×10^6 MC signal events, and B_i is taken from Eq. (1). We apply this fit for s and b to a $\pm 5\sigma$ region in ΔE and $M_{\rm inv}$, which has an acceptance (Ω) of 93.1%. There are a total of 54 events in this region, and, when s is constrained to be ≥ 0, the fit finds $s = 0.0$ and $b = 54.0$. The χ^2 of the fit projection in ΔE is 7.90 for 10 bins, while in $M_{\rm inv}$ it is 5.57 for 10 bins. These values correspond to confidence levels (evaluated via toy MC simulation) of 0.66 and 0.86, respectively.

To calculate the upper limit, Monte Carlo samples are generated by fixing the expected number of background events ($\tilde{b}$) to the value $b = 54$. For every assumed expected number of signal events ($\tilde{s}$), 10 000 samples are generated, for each of which the numbers of signal events and background events are determined by Poisson statistics with means of $\tilde{s}$ and $\tilde{b}$, respectively. We then assign ΔE and $M_{\rm inv}$ values to these events according to their density distributions. An unbinned maximum likelihood fit is performed for every sample to extract the number of signal events (s^{MC}). The confidence level for an assumed $\tilde{s}$ is defined as the fraction of the samples whose s^{MC} exceeds s. This procedure is repeated until we find the value of $\tilde{s}$ ($\tilde{s}_{90}$) that gives a 90% chance of s^{MC} being larger than s.

The resulting upper limit at 90% C.L. is $\tilde{s}_{90} = 5.1$ events. An upper limit on the branching fraction is obtained via the formula:

$$\mathcal{B}(\tau \to \mu\gamma) < \frac{\tilde{s}_{90}}{2(\epsilon\Omega)N_{\tau\tau}}, \qquad (3)$$

where $N_{\tau\tau}$ is the total number of τ pairs produced. Inserting the values $\tilde{s}_{90} = 5.1$, $\epsilon = 12.0\%$, $\Omega = 93.1\%$, and $N_{\tau\tau} = 7.85 \times 10^7$ gives $\mathcal{B}(\tau \to \mu\gamma) < 2.9 \times 10^{-7}$ [16].

To take into account systematic uncertainties related to $\tilde{s}_{90}$, $(1 + \Lambda)$ and κ are varied by $\pm 1\sigma$ each. This affects $\tilde{s}_{90}$ by $+0.06/-0.11$ events. The uncertainties in the functional forms of the background events are evaluated by varying the most sensitive parameters by their evaluated errors. The functional form is broadened or shortened by 1.2 or 0.8 times for $N^{\tau\tau\gamma}(M_{\rm inv}, \Delta E)$ and by 1.4 or 0.9 times for $N^{\not\mu\mu\gamma}(M_{\rm inv}, \Delta E)$, and their centers are shifted by ± 0.02 GeV for $N^{\tau\tau\gamma}(M_{\rm inv}, \Delta E)$ and by ± 0.015 GeV for $N^{\not\mu\mu\gamma}(M_{\rm inv}, \Delta E)$. These factors are about the largest that still give an acceptable fit to the background distributions. The shift of the central value for the $N^{\tau\tau\gamma}(M_{\rm inv}, \Delta E)$ spectrum yields the largest effect of ± 0.2 events, and the overall systematic uncertainty is evaluated as ± 0.3 events. The stability of the result as the fit region is varied is checked by extending the ΔE-$M_{\rm inv}$ region to $\pm 8\sigma$; $s = 0.0$ and $b = 105.0$ are obtained, and $\tilde{s}_{90}$ varies by only 0.07 events.

The systematic uncertainties on the detection sensitivity $2(\epsilon\Omega)N_{\tau\tau}$ arise from the track reconstruction efficiency (2.0%), photon reconstruction efficiency (2.8%), selection criteria (2.2%), luminosity (1.4%), trigger efficiency (1.6%), and MC statistics (0.8%). The total uncertainty is obtained by adding all of these components in quadrature; the result is 4.7%. This uncertainty is included in the upper limit on $\mathcal{B}(\tau \to \mu\gamma)$ following [6,18].

The angular distribution of the $\tau \to \mu\gamma$ decay essentially depends on the lepton flavor violation interaction structure [19], and spin correlations between the τ's at the signal and tagged sides must be considered. To evaluate the maximum possible variation, $V - A$ and $V + A$ interactions are assumed; no statistically significant difference in the ΔE-$M_{\rm inv}$ distribution or in the efficiency is found compared to the case of the uniform distribution.

The incorporation of all systematic uncertainties increases the upper limit by 6.3%, of which the effect of the $N_{BG}(M_{\rm inv}, \Delta E)$ uncertainty dominates. As a result, the upper limit on the branching fraction is

$$\mathcal{B}(\tau \to \mu\gamma) < 3.1 \times 10^{-7} \quad \text{at } 90\% \text{ C.L.} \qquad (4)$$

This result is lower than previous limits for this mode and helps constrain physics beyond the standard model.

We wish to thank the KEKB accelerator group for their excellent operation of the KEKB accelerator. We are grateful to J. Hisano, A. Ilakovac, and Y. Okada for fruitful discussions. We acknowledge support from the Ministry of Education, Culture, Sports, Science, and Technology of Japan and the Japan Society for the Promotion of Science; the Australian Research Council and the Australian Department of Education, Science and Training; the National Science Foundation of China under Contract No. 10175071; the Department of Science and Technology of India; the BK21 program of the Ministry of Education of Korea and the CHEP SRC program of the Korea Science and Engineering Foundation; the Polish State Committee for Scientific Research under Contract No. 2P03B 01324; the Ministry of Science and Technology of the Russian Federation; the Ministry of Education, Science and Sport of the Republic of Slovenia; the National Science Council and the Ministry of Education of Taiwan; and the U.S. Department of Energy.

*On leave from Nova Gorica Polytechnic, Nova Gorica.

[1] R. Barbieri and L. J. Hall, Phys. Lett. B **338**, 212 (1994); J. Hisano *et al.*, Phys. Lett. B **357**, 579 (1995); K. S. Babu, B. Dutta, and R. N. Mohapatra, Phys. Lett. B **458**, 93 (1999); S. F. King and M. Oliveira, Phys. Rev. D **60**, 035003 (1999).

[2] MARK-II Collaboration, K. G. Hayes *et al.*, Phys. Rev. D **25**, 2869 (1982).

[3] ARGUS Collaboration, H. Albrecht *et al.*, Z. Phys. C **55**, 179 (1992).

[4] DELPHI Collaboration, P. Abreu *et al.*, Phys. Lett. B **359**, 411 (1995).

[5] CLEO Collaboration, A. Bean *et al.*, Phys. Rev. Lett. **70**, 138 (1993); CLEO Collaboration, K.W. Edwards *et al.*, Phys. Rev. D **55**, R3919 (1997).
[6] CLEO Collaboration, S. Ahmed *et al.*, Phys. Rev. D **61**, 071101 (2000).
[7] BaBar Collaboration, C. Brown *et al.*, Nucl. Phys. (Proc. Suppl.) **123B**, 88 (2003).
[8] S. Kurokawa and E. Kikutani, Nucl. Instrum. Methods Phys. Res., Sect. B **499**, 1 (2003).
[9] Belle Collaboration, A. Abashian *et al.*, Nucl. Instrum. Methods Phys. Res., Sect. A **479**, 117 (2002).
[10] KORALB(v.2.4)/TAUOLA(v.2.6): S. Jadach and Z. Wąs, Comput. Phys. Commun. **85**, 453 (1995); S. Jadach, Z. Wąs, R. Decker, and J. H. Kühn, Comput. Phys. Commun. **64**, 275 (1991); **70**, 69 (1992).
[11] http://www.lns.cornell.edu/public/CLEO/soft/QQ
[12] CERN Program Library Long Writeup No. W5013, 1993.
[13] A. Abashian *et al.*, Nucl. Instrum. Methods Phys. Res., Sect. A **491**, 69 (2002).
[14] Belle Collaboration, K. Abe *et al.*, Phys. Lett. B **551**, 151 (2001).
[15] I. Narsky, Nucl. Instrum. Methods Phys. Res., Sect. A **450**, 444 (2000).
[16] Using the Bayesian approach described by the Particle Data Group [17], we obtain a 90% C.L. upper limit of 7.9 for the number of $\tau \to \mu\gamma$ events. Inserting this value into Eq. (3) along with $\epsilon = 12.0\%$, $\Omega = 87.3\%$ gives $\mathcal{B}(\tau \to \mu\gamma) < 4.8 \times 10^{-7}$.
[17] K. Hagiwara *et al.*, Phys. Rev. D **66**, 010001 (2002).
[18] The quantity $1/[2(\epsilon\Omega)N_{\tau\tau}]$ is integrated assuming a Gaussian distribution for $2(\epsilon\Omega)N_{\tau\tau}$.
[19] R. Kitano and Y. Okada, Phys. Rev. D **63**, 113003 (2001).